WELL TEST ANALYSES ON JATIBARANG VOLCANICS USING SINGLE WELL MODELLING

by
Thawer, R., Sarginson, M., Syahrial, E.

ABSTRACTS

Well test analyses on the Jatibarang Formation volcanics reservoir in the Jatibarang field were carried out using a numerical simulator with a single radial well model. The volcanics zone is a fractured reservoir with little matrix permeability. Conventional analytical methods for pressure build-up test analysis may be adapted to account for dual porosity and/or multiphase flow in a reservoir. However, vertical phase segregation, likely to occur with solution gas in a fractured reservoir, cannot be accounted for. In the current study, it was observed that the values of fracture permeability and the matrix - fracture coupling factor were derived were more realistic than those inferred from previous studies using conventional techniques. Three wells in the Jatibarang field were modelled in this way: the results indicate a fracture permeability in the range of 20mD to 150mD, fracture porosity between 0.03% to 0.12% and (also known as the matrix shape factor) between 1 and 14. Build-up data from the three wells are documented to allow further analyses and comparisons using advanced analytical techniques in future.

It is recommended that the reservoir description of the Jatibarang Formation be reviewed, using current log and well test analyses techniques. The reservoir engineering simulation model should then be updated to incorporate the new description.

I. INTRODUCTION

The Jatibarang field is situated 30 km northwest of Cirebon in West Java (Fig. 1). It lies near the eastern end of the Northwest Java Basin. The major producing zone is the Jatibarang Formation volcanics (Fig. 2), a sequence of tuffs and lavas which are of Eocene to Oligocene age. The volcanics reservoir occupies a culmination on a major east-west trending anticline and is bounded by two major faults to the east and west (Fig. 3).

Oil and solution gas are produced from the volcanics zone. Flow in the reservoir is thought to occur via natural fractures. Most of the wells producing from the volcanics are barefoot completions, commonly producing from over 100m of open hole. Previous studies have used conventional analysis of well test pressure build-up data to obtain values for fracture permeability and matrix-fracture coupling (). It was felt that these analyses did not yield results that correlated with core data and drilling experience. The values of fracture permeability and derived did not seem large enough to result in the lost circulation during the drilling of most of the wells into the volcanics, despite the extremely low permeability of the matrix rock. Part of the problem in previous analyses may have been due to inhomogeneity of the reservoir near the wells (e.g. shale breaks, faulting). Another complication may have been three-phase flow and vertical segregation, which cannot be accounted for in conventional analytical solutions. This prompted the study using a numerical model, in which these complications could be incorporated.

After reviewing all the test data from the field, build-up tests from three wells, JTB-105, JTB-175, and JTB-190, were identified as being of long enough duration for both fractures and matrix to have significant effects. These were therefore selected for single well modelling.

with the objective of obtaining more realistic values for fracture permeability and porosity, and matrix-fracture coupling.

II. POROSITY TYPES IN THE VOLCANICS

Core data were not available for any of the wells under study. Two cores were taken in well JTB-113, 1.1km northeast of JTB-190 (Fig. 3), and a full set of core plugs was available from these. XRD analysis and thin sections, made from selected plugs, show that the lithology in JTB-113 is felsic tuff. Most of the porosity visible is solution porosity, resulting from leaching of feldspar phenocrysts (Fig. 4, Fig. 5). Microfractures are also present (Fig. 4), but most of their porosity has been infilled by chlorite and quartz mineralisation. Microporosity is locally present in the groundmass (Fig. 5). Core analysis yielded porosity values ranging from 1% to 22% (average 10%). Measured permeabilities are low, generally less than 0.1mD, indicating that matrix permeability must be very low.

III. LOG ANALYSIS

Comparison of log responses in the volcanics section in JTB-113 with the wells under study suggests that the lithology in all four wells is similar (Figs. 6 - 9). XRD analysis of JTB-113 core plugs shows that the major constituents are alkali feldspar (sanidine) and quartz. Lesser amounts of clay minerals (chlorite and illite-smectite) and plagioclase feldspar (oligoclase) are also present.

Porosity was calculated at 0.25m depth intervals using a three mineral model: clay, alkali feldspar, and quartz+plagioclase (the log responses of quartz and oligoclase are sufficiently similar for them to be treated together as one component). The method used is explained in detail in Doveton, 1986, Chapter 6. Linear equations relating log response to mineral proportions were set up for each porosity log:-

Bulk Density:

$$RHOB = RHOB_{CL}.V_{CL}+RHOB_{AF}.V_{AF}+RHOB_{QP}.V_{QP}+RHOB_{FL}.POR$$

Neutron Porosity:

$$NPHI = NPHI_{CL}.V_{CL}+NPHI_{AF}.V_{AF}+NPHI_{QP}.V_{QP}+NPHI_{FL}.POR$$

Gamma Ray:

$$GR = GR_{CL}.V_{CL}+GR_{AF}.V_{AF}+GR_{QP}.V_{QP}+GR_{FL}.POR$$

Unity Equation:

$$1=V_{CL}+V_{AF}+V_{QP}+POR$$

...where V_{CL}, V_{AF}, V_{QP}, POR are the proportions of clay, alkali feldspar, quartz+plagioclase, and porosity (these should sum to 1, yielding the unity equation); $RHOB_{CL}$, $RHOB_{AF}$ etc. are the log responses for each of these components.

This set of simultaneous equations was then converted into matrix form:

$$\begin{pmatrix} RHOB \\ NPHI \\ GR \\ 1 \end{pmatrix} = \begin{pmatrix} RHOB_{CL} & RHOB_{AF} & RHOB_{QP} & RHOB_{FL} \\ NPHI_{CL} & NPHI_{AF} & NPHI_{QP} & NPHI_{FL} \\ GR_{CL} & GR_{AF} & GR_{QP} & GR_{FL} \\ 1 & 1 & 1 & 1 \end{pmatrix} \begin{pmatrix} V_{CL} \\ V_{AF} \\ V_{QP} \\ POR \end{pmatrix}$$

...which in matrix notation may be expressed as:

$$\mathbf{L} = \mathbf{CV}$$

This can be solved to obtain the mineral proportions and porosity contained in matrix **V** by multiplying the log response matrix **L** by the inverse of the component log response matrix **C** :

$$\mathbf{V} = \mathbf{C}^{-1}\mathbf{L}$$

The mineral log responses in matrix **C** may be treated as constants. Standard values were used for alkali feldspar and quartz density and neutron porosity. Alkali feldspar gamma ray was estimated from the maximum gamma reading (corrected for borehole effects) in the area under study. Clay parameters were estimated from the shale section immediately overlying the volcanics. The pore fluid was taken to be fresh water, which gives approximately the same response as the brackish mud filtrate with low residual oil saturation actually present in the invaded zone in the volcanics. Log analysis parameters are listed in Table 1.

If the mineral model used is inaccurate (e.g. due to the presence of additional minerals), the above method may yield negative proportions. Occasional errors of this sort were noted. To optimize the model used, the component gamma ray responses were varied until values yielded a minimum sum of negative proportions for each well. The gamma ray response equation is probably the least accurate, because the gamma response may be significantly affected by radioactive accessory minerals and uranium in the formation. Spectral gamma was not run in any of the wells studied.

This method was initially tried out for well JTB-113. Calculated porosities were in close agreement with measured core porosities. Water saturation was calculated using the Indonesia equation, with standard values for the Archie parameters (a=1, m=2, n=2). Log analysis results are shown in Figures 6, 7, and 8. Calculated average porosities for JTB-105, JTB-175, and JTB-190 are 8.3%, 8.9%, and 11.9% respectively, with water saturations of 58.5%, 55.8%, and 52.0%.

An LDT was run in JTB-190, and the PEF curve from this was incorporated the porosity/lithology calculation to give more accurate lithology determination. Because of the extra response equation for PEF the lithology model for this well was overdetermined, and the log response equations were solved using a least-squares best fit. In matrix form this is:

$$V = (C^T C)^{-1} C^T L$$

Because each porosity log is scaled in different units, the log response equations were normalized for this well, so that the range of mineral response coefficients was roughly the same for each equation, before calculating the best fit. Thus the result was not biased towards logs scaled in higher units, such as the gamma ray. The weighting factors used were 1/1.71 for RHOB, 1 for NPHI, 1/500 for GR, and 1/10 for PEF. The unity equation was given an arbitrarily high weighting of 100, to ensure that the calculated proportions summed to one for each depth interval.

IV. GEOLOGICAL MODELS

Seismic data were not available for the current study, so geological interpretation in the area of interest was based on well data only. Structural dips appear to be low (less than 7 degrees, typically 3 - 4 degrees) near the wells modelled, so the top of the volcanics was treated as being horizontal in each model. Well log interpretation indicated a shale break within the volcanics in wells JTB-105 and JTB-175 (Figs. 10 and 12); this was correlated with the surrounding wells (Fig. 13), and incorporated into the single well models as a transmissibility barrier, horizontally covering the whole area of each model. The thickness of this shale break is between 6m and 15m in the vicinity of the two wells under study. The presence of a fault in the vicinity of JTB-190 was inferred from missing section in the Talang Akar Formation overlying the volcanics, the "U" sandstone being absent in this well (Fig. 14). The missing section was calculated to be 54m, implying a similar vertical displacement on the fault, down-faulting Talang Akar Formation shales against the volcanics. This was incorporated in the single well model by setting the blocks corresponding to downthrown Talang Akar shales as inactive. Some minor faults shown on the top volcanics map (Fig. 3) are not shown on the cross sections (Figs. 13 and 14) and were not modelled. Porosities calculated from log analysis were incorporated into each model. In the case of JTB-190, log analysis results indicated little variation in porosity in the volcanics section, so an average value was used for all the grid blocks. For wells JTB-105 and JTB-175 more variation in porosity was evident, so model layers were based on log character, and assigned corresponding calculated porosities.

V. NUMERICAL MODELS

The geological model for each well was translated into a radial segmented numerical model in ECLIPSE. Matrix porosities were obtained from the log analyses of the wells. Since reservoir core was not available for these wells, first estimates of the matrix permeabilities were taken from core analyses done (LEMIGAS and Core Laboratories Inc. 1975) on core from the same formation in a nearby well (JTB-113). These were subsequently tuned to infer the matrix permeability from history matching the well test data. Fracture permeability, fracture porosity and (from Kazemi's numerical model, which used the matrix - fracture shape factor to allow flow calculations between matrix and fracture) were also used as tuning parameters. The model was run in a dual permeability and dual porosity mode allowing flow between matrix blocks as well as between the fracture and matrix systems. Build-up data recorded in the field for the three wells studied are presented in Table 2. A cross section of the radial well model in Fig. 15 illustrates the different pressure response in the matrix blocks and the surrounding fracture system from one time step to another during production prior to shut-in and build-up testing. The ECLIPSE input data file for JTB-105 is included in Appendix 1.

VI. DISCUSSION OF RESULTS FROM THE HISTORY MATCHING

The history matched results for the three wells are displayed in Figs. 16, 17 and 18. The early time data is obscured by well-bore storage and should be ignored.

The fracture and matrix permeabilities, porosities and sigmas for the best matches are compared with results from conventional analyses done previously (LEMIGAS report, 1988), and with properties derived from log analysis, in Table 3. The numerical model implies a larger fracture permeability and a higher degree of fracturing than conventional techniques. We also observed that the core-derived matrix permeabilities were too high to provide a good match, and these were subsequently tuned down.

Current results corroborate the speculations on reasons for the losses in circulation observed whilst drilling most of the wells into the volcanics. They would also help to correct the inexplicably large fracture permeabilities used to compensate a low value employed in previous reservoir simulation studies, because oil production rates could not be matched using the fracture permeabilities inferred from previous well test analyses.

To get an idea of the implications for fracture geometry of these results, values for fracture spacing and fracture width were calculated based upon the best fit values of fracture porosity and σ. Fracture spacing and may be related via Kazemi's equation:

$$\sigma = 4\left(\frac{1}{dx^2}+\frac{1}{dy^2}+\frac{1}{dz^2}\right)$$

...where dx, dy, and dz are the fracture spacings in the x, y, and z directions.

If a "cube" model is assumed (i.e. three orthogonal sets of equally spaced identical parallel fractures), then this equation reduces to:

$$\sigma = \frac{12}{d^2} \qquad \text{therefor } d = \frac{\sqrt{12}}{\sigma}$$

...where d is the fracture spacing in metres.

If a "slab" model is assumed (i.e. identical parallel evenly spaced fractures) then the Kazemi equation gives:

$$\sigma = \frac{4}{d^2} \qquad \text{therefor } d = \frac{2}{\sqrt{\sigma}}$$

Substitution of best fit values of into these equations values yielded implied fracture spacings of between 1.7

and 3.5 metres for the cube model, or between 1 and 2 metres for the slab model.

For the cube model, the equation relating fracture porosity to fracture spacing and width is:

$$\Phi_F = 1 - \left(\frac{d}{d+w}\right)^3 \qquad \text{so } w = d\left[(1-\Phi_F)^{-1/3} - 1\right]$$

...where F is the fracture porosity (fractional), and w is the fracture width in metres.

For the slab model, the corresponding equation is:

$$\Phi_F = \frac{w}{d+w} \qquad \text{therefor } w = \frac{d \,.\, \Phi_F}{1-\Phi_F}$$

Using these equations with the best fit values of fracture porosity, fracture widths of between 0.2 and 0.8 mm were calculated for the cube model, and between 0.4 and 1.4 mm for the slab model. Results of these calculations for all three wells are shown in table 4.

Microfractures seen in the core samples from JTB-113 were typically about 0.1 mm in diameter, ranging up to 0.5 mm. Thus the fracture widths implied by the models are in reasonably close agreement with observation. The slightly higher fracture widths calculated from the JTB-175 best fit may indicate the presence of larger fractures (than those seen in core plugs) and/or vugs connected to the fracture system. Thin sections from JTB-113 show evidence to support the latter hypothesis:- secondary porosity is commonly developed in leached feldspar crystals adjacent to microfractures. When two or three phase flow occurs, some of these pores may be by-passed as dead ends. This needs to be reflected in the recovery mechanism, and is best introduced as adjustments on the relative permeability curves for the fractures.

The distance between microfractures seen in thin sections is generally a few mm; two orders of magnitude smaller than the inter-fracture distances implied by the models. However most of the microfractures seen were sealed (with quartz and chlorite mineralisation), whereas the inter-fracture distance calculated from the models reflects the spacing between open fractures only.

The fracture spacings and widths implied by the values of fracture porosity and used in a previous simulation model are also shown in Table 4. It is evident that both the fracture spacings (more than 600 m) and widths (more than 5 m) are unfeasibly large.

VII. SENSITIVITY STUDIES

In the absence of direct measurements of fracture permeability and porosity, it is useful to observe the interaction of these two parameters for future reservoir history matching studies. It was observed for our wells that when the two were varied inversely the only observed difference lay in the early time build-up. This means that near well reservoir pressure draw-down could be matched by a straight swap between the two, everything else being equal, except during early build-up time when well-bore storage affects pressure build-up and therefore does not allow us to distinguish the difference between the two parameters. Fracture permeability and porosity are thus interchangeable since absolute values in practice could not be assigned to either. This interdependency was useful in allowing us to constrain and focus the tuning in subsequent history matching on full field reservoir studies. Figure 19 is an illustration of such a direct swap. Ideally fracture porosity should be measured using current advanced logging tools, leaving fracture permeability as a parameter for tuning.

A similar relationship was observed between sigma and matrix permeability at very low values of matrix permeability. Matrix permeability values of less than 0.001 mD could be varied inversely with sigma causing no change in the build-up curve. A change in sigma alone changes the shape of the build up curve with very little movement of the end points (Fig. 20). At higher values of matrix permeability the shape and the position of the curve changed as would be expected from a change in sigma together with a change in the total permeability of the system. Figure 21 is an illustration of such a swap. The increase in matrix permeability led to a very small shift in the pressure curve indicating a small flow contribution from the matrix. The response was equivalent to a fractional increase in the fracture permeability. These observations led us to believe that it was possible to approximate a dual permeability-dual porosity model for very low matrix permeability formations by using dual porosity only and adjusting sigma and fracture permeabilities/porosities.

The above two relationships will serve to reduce significantly expensive computer run time for full field reservoir simulation studies. Care should be exercised when swapping matrix permeability for sigma, because this is only valid at very low values of matrix permeability.

Finally, it should be noted that the inferred reservoir pressure from these studies was higher than that from previous analyses on all the three wells. These results will provide a starting point for building a new reservoir model for Jatibarang.

VIII. CONCLUSIONS

1. With the help of reservoir geology based on current log analyses, single well numerical models with a radial geometry were built for JTB-105, JTB-175 and JTB-190. History matching of well tests was successfully completed.
2. Results have revealed sigma, fracture and matrix volumetrics/flow properties very different from previous studies and in line with current interpretations of the reservoir geology.
3. Sensitivity studies on the interplay of reservoir flow properties have revealed relationships that will increase efficiency in future full field simulation studies on Jatibarang.

IX. RECOMMENDATIONS

1. The log analyses of all the wells in Jatibarang need reviewing.
2. The general reservoir geology needs updating.
3. The well-test analyses in all wells need to be updated.
4. An updated simulation model should be built for Jatibarang incorporating current interpretations in the reservoir description.

ACKNOWLEDGMENT

We wish to thank Management and Staff of PERTAMINA UEP III, Management and Staff of DIVISI JIANTEK EP of PERTAMINA UEP III and also Dr. Brian Hackman for his invaluable help in editing and producing the final version of this report.

REFERENCES

Aguilera, R., 1980, *Naturally fractured reservoirs*, Penn Well Books, Tulsa.

Cox, K.G., Price, N.B., and Harte, B., 1974, "The practical study of crystals, minerals, and rocks": McGraw-Hill, Maidenhead, 245p.

Deer, W.A., Howie, R.A., and Zussman, J., 1966, *An introduction to the rock forming minerals*, Longman, London, 528p.

Doveton, J.H., 1986, *Log analysis of subsurface geology*, Wiley-Interscience, New York, 273p.

Elf Aquitaine Indonésie, 1992, "Feasibility study of a pilot horizontal well, Jatibarang field: Phase I and phase II geologic study": *Report for PERTAMINA UEP-III*, Cirebon, Indonesia.

Kazemi, H., 1976, "Pressure transient analysis of naturally fractured reservoirs with uniform fracture distribution", 2 SPEJ, June, 117-22; Trans., AIME, 261.

LEMIGAS and Core Laboratories Inc., 1975, "Reservoir evaluation of the volcanics formation, Jatibarang field": *Report for PERTAMINA UEP-III*, Cirebon, Indonesia.

LEMIGAS, 1988, "Studi optimalisasi produksi minyak Lapangan Jatibarang dan sekitarnya: simulasi

together with a change in the total permeability of the system. Figure 21 is an illustration of such a swap. The increase in matrix permeability led to a very small shift in the pressure curve indicating a small flow contribution from the matrix. The response was equivalent to a fractional increase in the fracture permeability. These observations led us to believe that it was possible to approximate a dual permeability-dual porosity model for very low matrix permeability formations by using dual porosity only and adjusting sigma and fracture permeabilities/porosities.

The above two relationships will serve to reduce significantly expensive computer run time for full field reservoir simulation studies. Care should be exercised when swapping matrix permeability for sigma, because this is only valid at very low values of matrix permeability.

Finally, it should be noted that the inferred reservoir pressure from these studies was higher than that from previous analyses on all the three wells. These results will provide a starting point for building a new reservoir model for Jatibarang.

VIII. CONCLUSIONS

1. With the help of reservoir geology based on current log analyses, single well numerical models with a radial geometry were built for JTB-105, JTB-175 and JTB-190. History matching of well tests was successfully completed.
2. Results have revealed sigma, fracture and matrix volumetrics/flow properties very different from previous studies and in line with current interpretations of the reservoir geology.
3. Sensitivity studies on the interplay of reservoir flow properties have revealed relationships that will increase efficiency in future full field simulation studies on Jatibarang.

IX. RECOMMENDATIONS

1. The log analyses of all the wells in Jatibarang need reviewing.
2. The general reservoir geology needs updating.
3. The well-test analyses in all wells need to be updated.
4. An updated simulation model should be built for Jatibarang incorporating current interpretations in the reservoir description.

ACKNOWLEDGMENT

We wish to thank Management and Staff of PERTAMINA UEP III, Management and Staff of DIVISI JIANTEK EP of PERTAMINA UEP III and also Dr. Brian Hackman for his invaluable help in editing and producing the final version of this report.

REFERENCES

Aguilera, R., 1980, *Naturally fractured reservoirs, Penn* Well Books, Tulsa.

Cox, K.G., Price, N.B., and Harte, B., 1974, "The practical study of crystals, minerals, and rocks": McGraw-Hill, Maidenhead, 245p.

Deer, W.A., Howie, R.A., and Zussman, J., 1966, *An introduction to the rock forming minerals*, Longman, London, 528p.

Doveton, J.H., 1986, *Log analysis of subsurface geology*, Wiley-Interscience, New York, 273p.

Elf Aquitaine Indonésie, 1992, "Feasibility study of a pilot horizontal well, Jatibarang field: Phase I and phase II geologic study": *Report for PERTAMINA UEP-III*, Cirebon, Indonesia.

Kazemi, H., 1976, "Pressure transient analysis of naturally fractured reservoirs with uniform fracture distribution", 2 SPEJ, June, 117-22; Trans., AIME, 261.

LEMIGAS and Core Laboratories Inc., 1975, "Reservoir evaluation of the volcanics formation, Jatibarang field": *Report for PERTAMINA UEP-III*, Cirebon, Indonesia.

LEMIGAS, 1988, "Studi optimalisasi produksi minyak Lapangan Jatibarang dan sekitarnya: simulasi reservoar struktur Jatibarang (lapisan vulcanic)": *Report for PERTAMINA UEP-III*, Cirebon, Indonesia.

Morrow, N.R., Brower, K.R., Shouxiang Ma, and Buckley,J.S., 1990, "Fluid flow in healed tectonic fractures": *Journal of Petroleum Technology*, October 1990, p.1310.

Nutt, W.L., and Jujur Sirait, 1985, "Application of offset seismic profiles in the Jatibarang volcanic reservoir": *Proceedings of the Indonesian Petroleum Association 14th Annual Convention*, Vol.2, p.385-406.

Schlumberger, 1991, "Log interpretation charts".

Soewono and Setyoko., 1987, "Application of the dual porosity concept for well log interpretation of Jatibarang volcanic tuff": *Proceedings of the Indonesian Petroleum Association 16th Annual Convention*, Vol.2, p.87-106.

Vernik, L., 1990, "A new kind of reservoir rock in volcaniclastic sequences": *Bulletin of the American Association of Petroleum Geologists*, Vol.74, No.6, p.830.

Table 1. Log analysis parameters

WELL No.	JTB-105	JTB-175	JTB-190
POROSITY LOGS	FDC-SNP-GR	FDC-CNL-GR	LDL-CNL-GR
RESISTIVITY LOG	SIES-PML-ML	ISF-MSFL	ISF-MSFL
BULK DENSITY (SG):			
Clay	2.6	2.6	2.6
Alkali Feldspar	2.52	2.52	2.52
Quartz	2.64	2.64	2.64
Pore Fluid	1	1	1
NEUTRON POROSITY (PU):			
Clay	39	35	33
Alkali Feldspar	-2	-3	-3
Quartz	-1	-2	-2
Pore Fluid	1	1	1
GAMMA RAY (API):			
Clay	130	130	130
Alkali Feldspar	300	280	300
Quartz	0	0	20
Pore Fluid	0	0	20
PEF (barns/electron):			
Clay	-	-	5.11
Alkali Feldspar	-	-	2.86
Quartz	-	-	1.89
Pore Fluid	-	-	0.358
RESISTIVITY (ohm.m):			
Rw @ 27C	0.22	0.23	0.22
Rclay @BHT	2	3	3

Table 2. Measured data during well-test pressure build-up

JTB-105 (dated 4/6/85) oil rate = 1m^3/day from zone 2209m to 2310m.		JTB-175 (dated 3/7/85) oil rate = 1m^3/day from zone 2075m to 2086m.		JTB-190 (21/8/85) oil rate = 2m^3/day from zone 2010m to 2165m.	
TIME hours	PRESSURE psi	TIME hours	PRESSURE psi	TIME hours	PRESSURE psi
0.000	1878.20	0.000	1072.16	0.000	1148.54
0.008	1897.26	0.016	1088.66	0.050	1150.39
0.016	1911.34	0.050	1130.76	0.116	1152.38
0.050	1922.72	0.083	1186.80	0.250	1154.23
0.116	1929.12	0.170	1235.16	0.500	1169.45
0.250	1934.24	0.250	1250.88	1.000	1292.62
0.500	1939.36	0.500	1263.18	1.500	1317.23
1.000	1943.2	1.000	1275.84	2.000	1321.07
2.500	1944.48	2.000	1282.24	3.500	1324.77
3.500	1947.04	3.500	1288.92	5.500	1326.76
5.500	1949.46	5.500	1300.16	8.500	1330.46
8.500	1953.3	8.500	1315.38	12.50	1335.83
12.50	1958.42	12.50	1333.16	17.50	1345.68
17.50	1963.54	17.50	1353.64	23.50	1355.21
23.50	1969.94	23.50	1373.98	30.50	1368.43
30.50	1975.06	30.50	1396.88	36.50	1375.97
38.50	1982.13	38.50	1421.06		
46.50	1987.72	48.00	1442.68		
54.50	1994.12				
60.00	1997.96				

Table 3. Results of the current study compared with previous analyses

Well name	JTB-105			JTB-175			JTB-190		
Source of data	Log analysis	Previous field model	Current well model	Log analysis	Previous field model	Current well model	Log analysis	Previous field model	Current well model
Matrix porosity (%)	5 to 10	12.35	**5 to 10**	4.7 to 10.1	10.91	**4.7 to 10.1**	11.9	13.72	**11.9**
Matrix permeability (mD)	N/A	2.08	**0.002 to 0.001**	N/A	1.9	**0.005**	N/A	13.4	**0.002**
Fracture porosity (%)	N/A	1.36	**0.02**	N/A	1.42	**0.1**	N/A	0.87	**0.04**
Fracture permeability (mD)	N/A	16300	**148**	N/A	16800	**150**	N/A	49800	**50**
$\sigma(m^{-2})$	N/A	0.00001	**1.0**	N/A	0.00001	**2**	N/A	0.00001	**4**
Reservoir pressure (barsa)	N/A	154	**146**	N/A	138	**135**	N/A	103	**125**

Table 4. Fracture spacing and width calculated using model values σ and fracture porosity

Well name	JTB-105		JTB-175		JTB-190	
Source of data	Previous field model	Current well model	Previous field model	Current well model	Previous field model	Current well model
Fracture porosity (%)	1.36	**0.02**	1.42	**0.1**	0.87	**0.04**
$\sigma(m^{-2})$	0.00001	**1**	0.00001	**2**	0.00001	**4**
Implied fracture spacing (m): - Cube	1100	**3.5**	110	**2.4**	1100	**1.7**
Implied fracture spacing (m): - Cube	630	**2.0**	630	**1.4**	630	**1.0**
Implied fracture width (m): - Cube	5000	**0.23**	5200	**0.82**	3200	**0.23**
Implied fracture width (m): - Cube	870	**0.40**	9100	**1.4**	5600	**0.40**

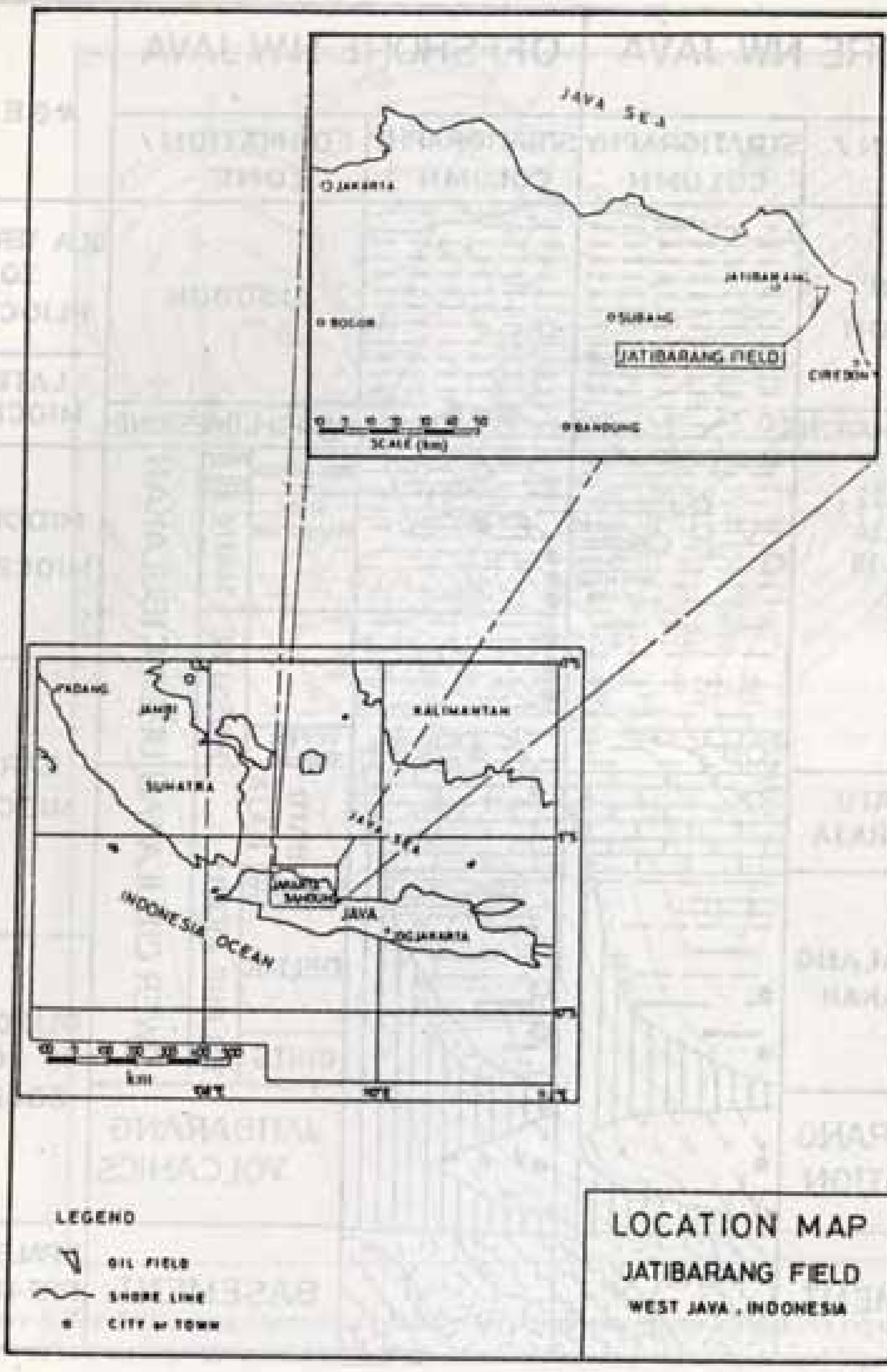

Figure 1. (From Nutt and Jujur Sirait, 1987)

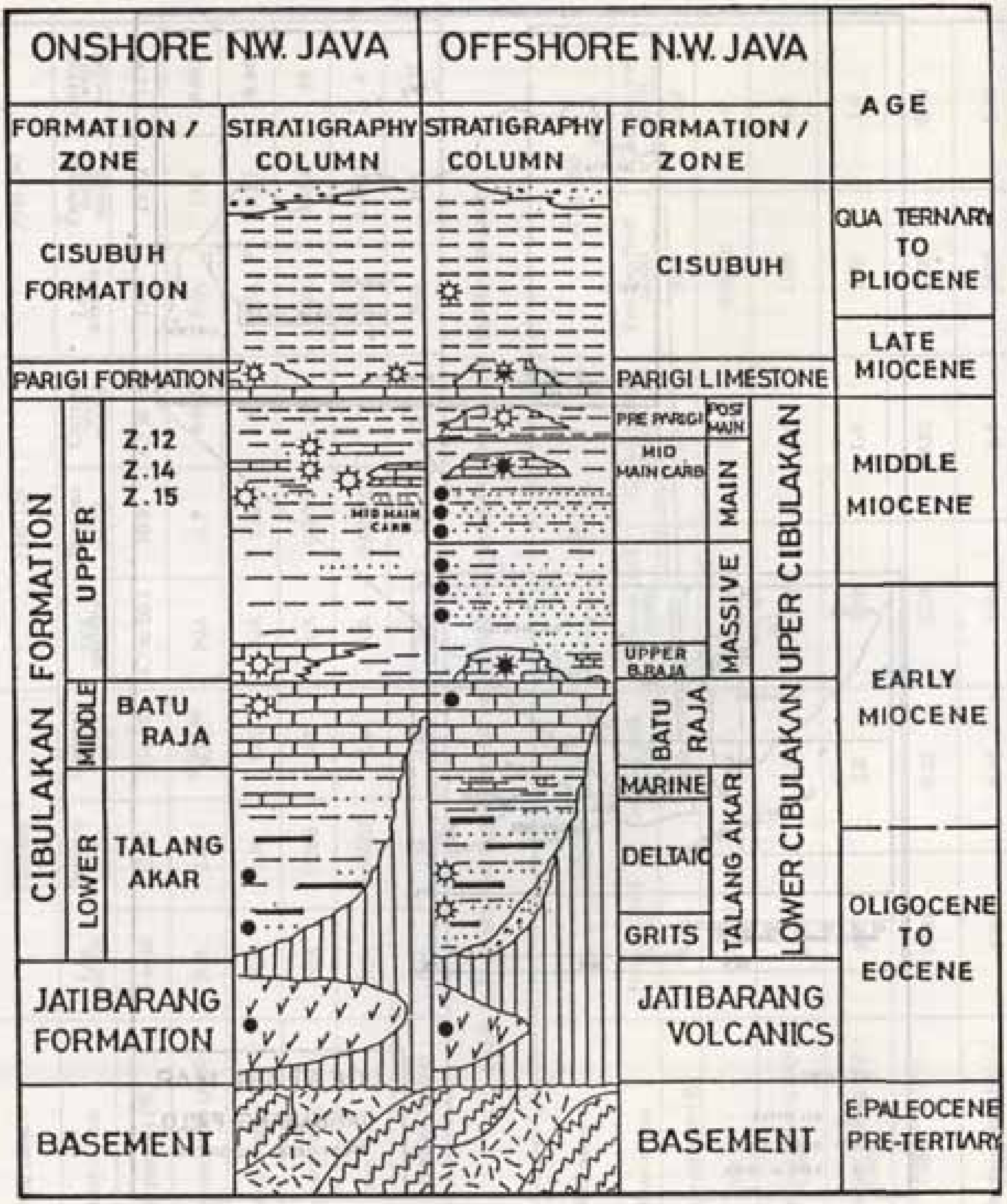

Figure 2. Stratigraphy of the NW Java basin (from Soewono and Setyoko, 1987)

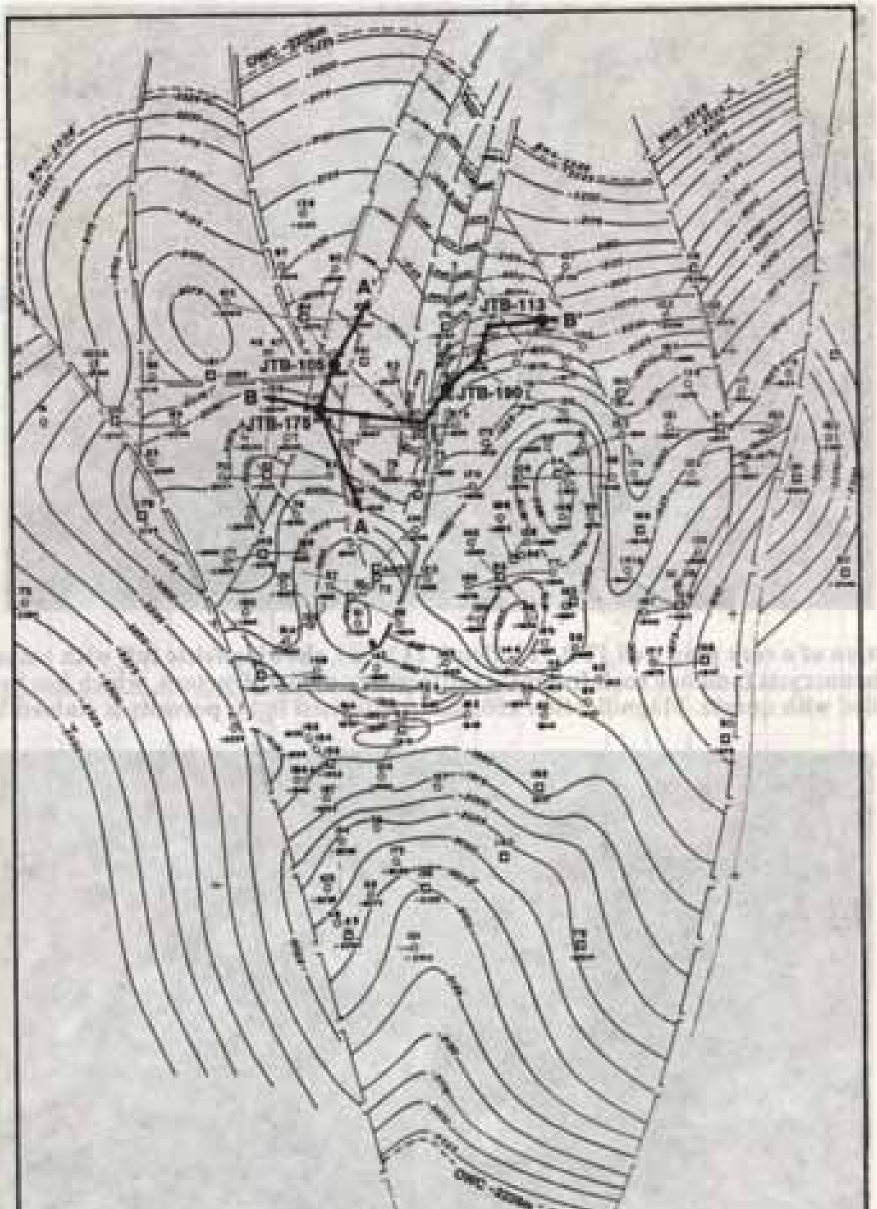

Figure 3. Top Jatibarang Formation volcanics structure map (from LEMIGAS report, 1988) A – A' and A – B' are the lines of the cross sections shown in Fig. 13 and Fig. 14.

Fig. 4 Thin section of a core plug well JTB-113 (depth 2120 m), showing felsic tuff with porosity in leached feldspsr phenocrysts (and one rock fragment) adjacent to a microfracture, which has been largely infilled with quartz. Magnification x50, plane polarized light; porosity is stained blue

Fig. 5 Thin section of a core plug from well JTB - 113 (depth 2132 m), showing felsic tuff with porosity developed in leached feldspsr phenocrysts. Some microporosity is present in the groundmass. Magnification x50, plane polarized light; is stained blue

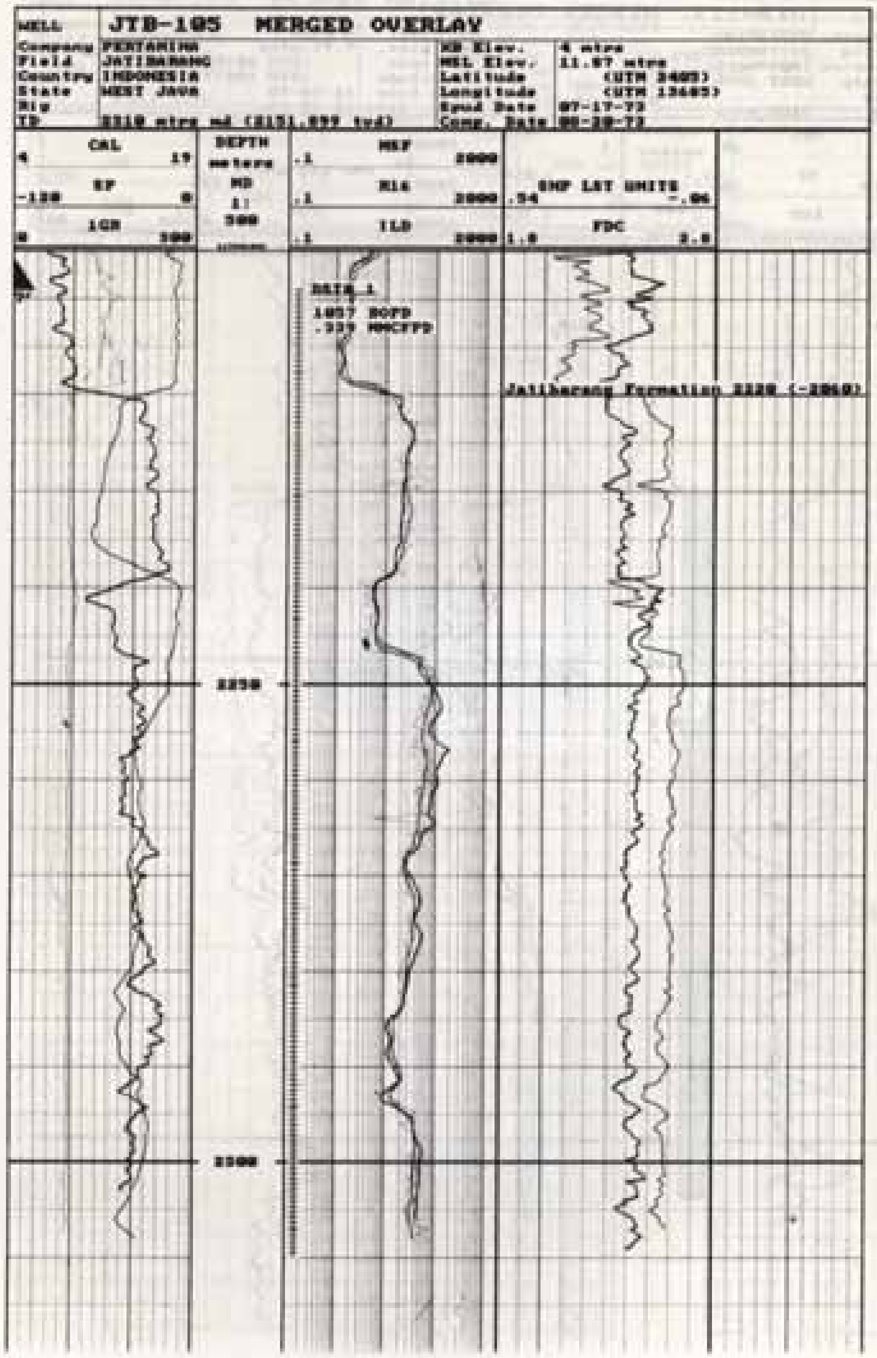

Figure 6. JTB – 105 logs.

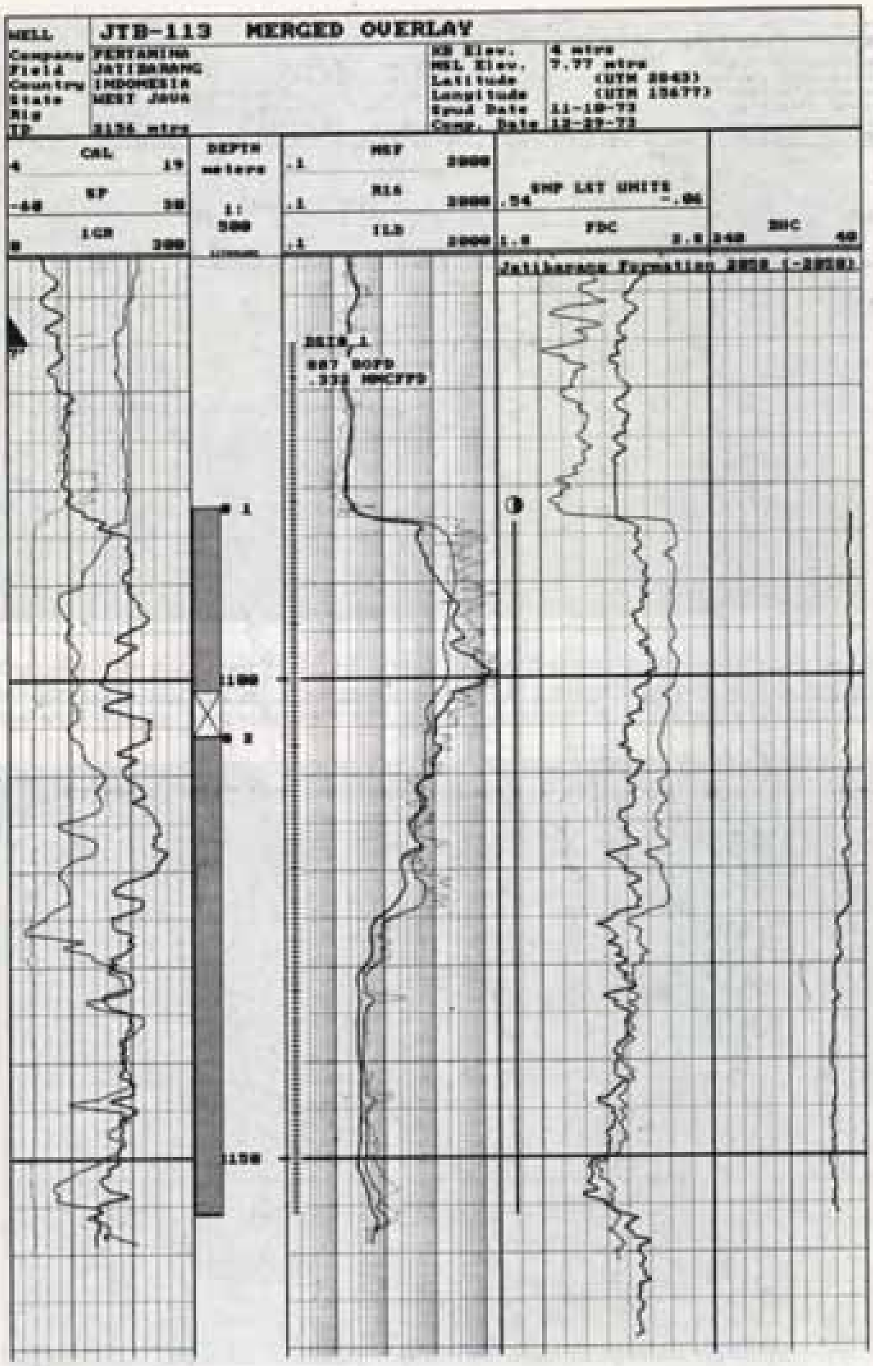

Figure 7. JTB – 113 logs.

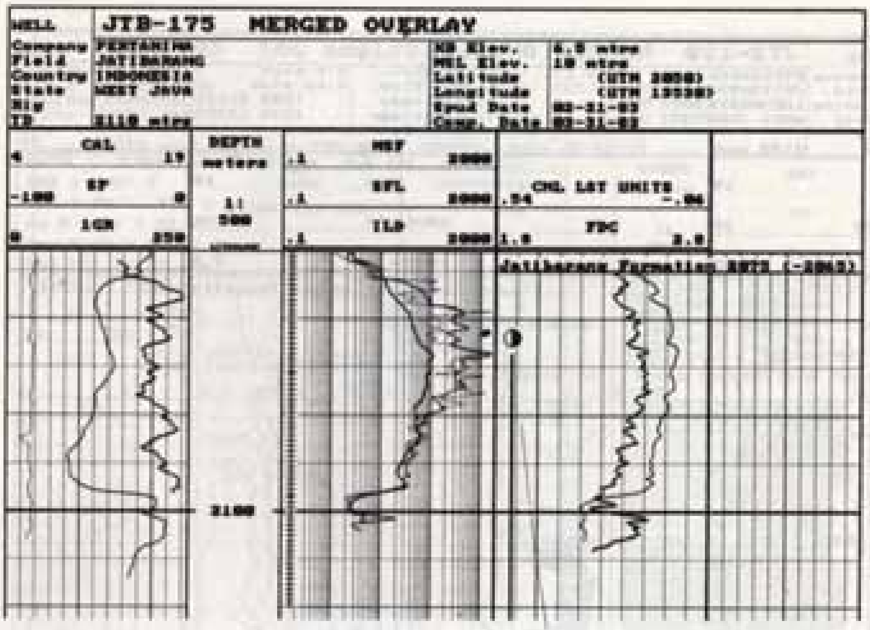

Figure 8. JTB – 175 logs.

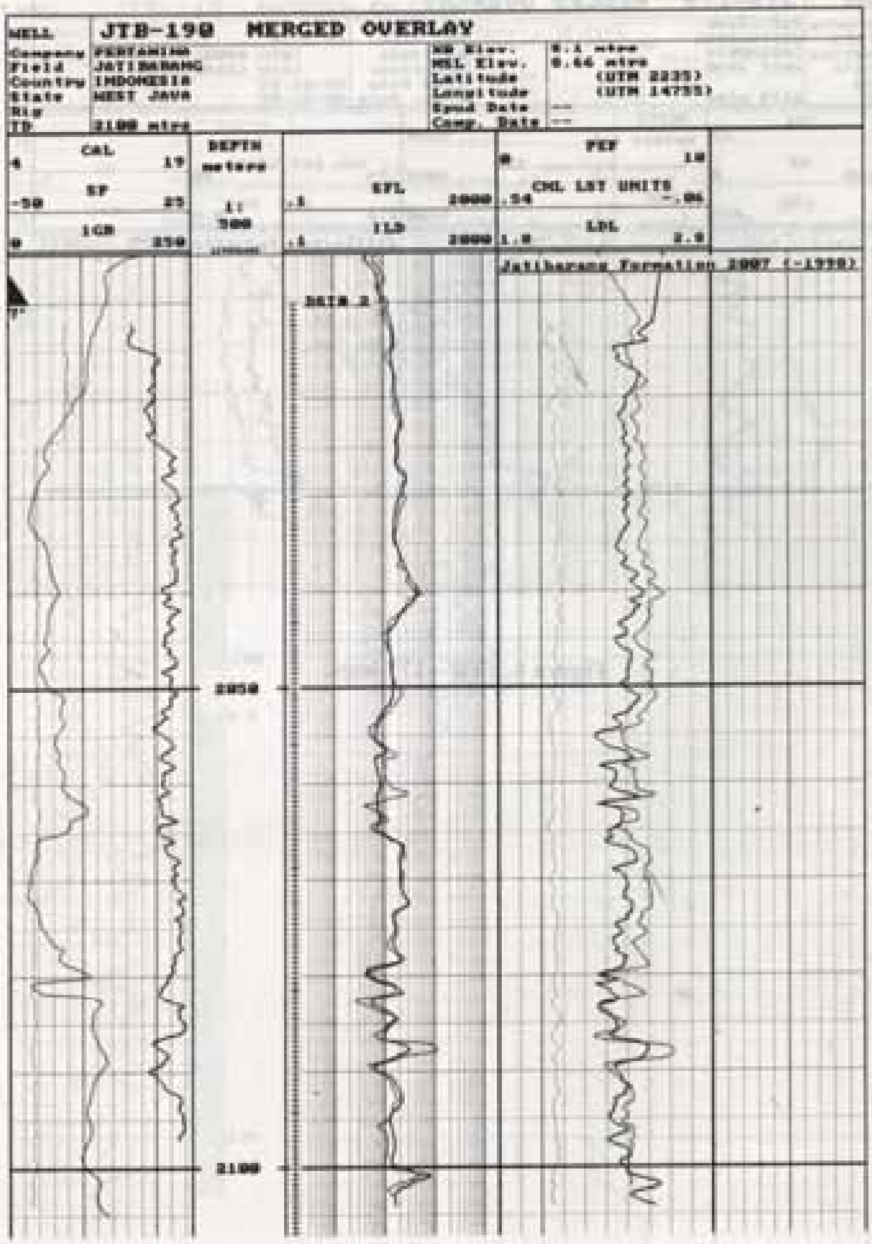

Figure 9. JTB – 190 logs

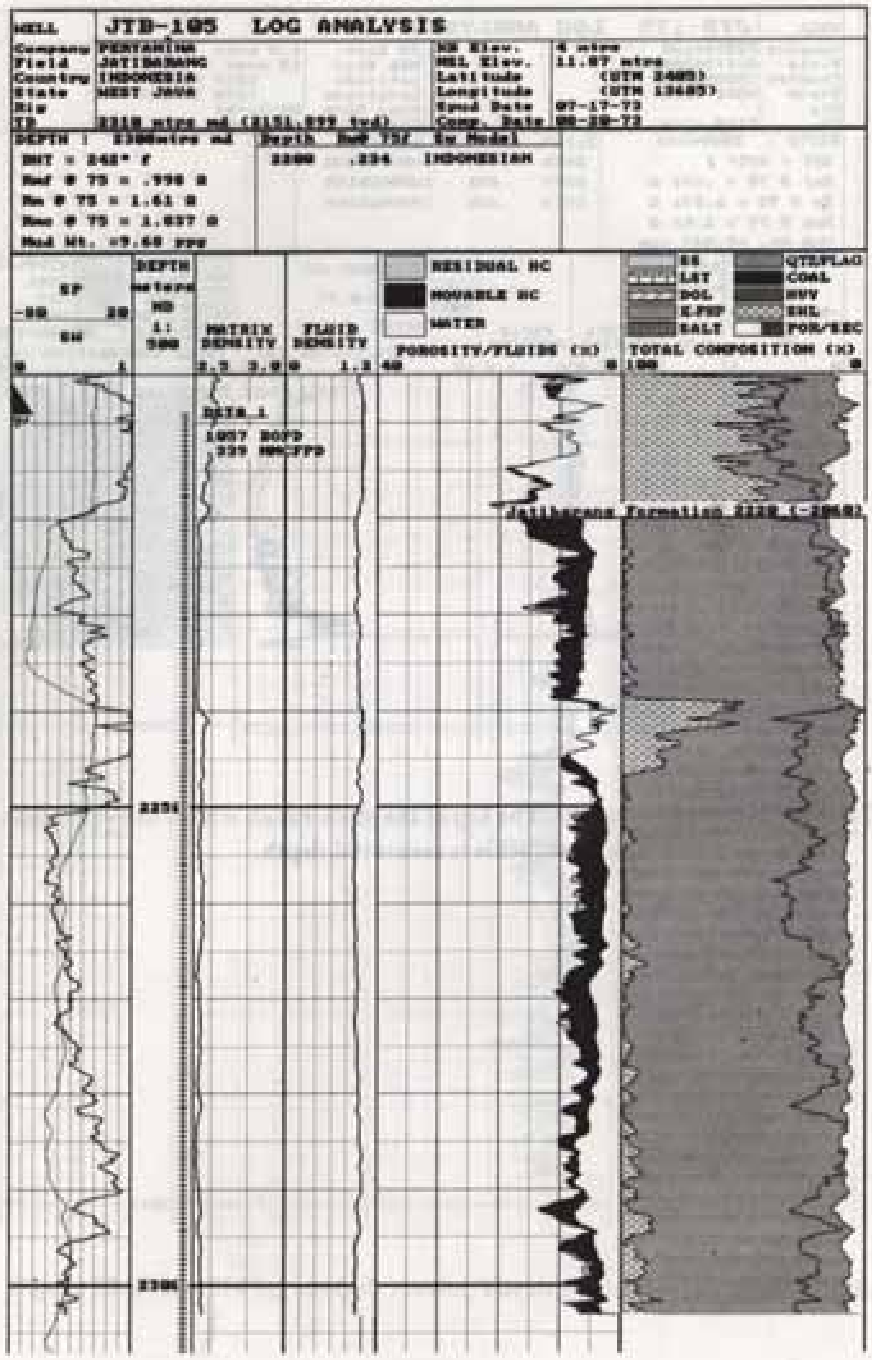

Figure 10. JTB – 105 log analysis results. The shale break within the volcanics lies between 2239 and 2246 m. The depth scale is measure depth.

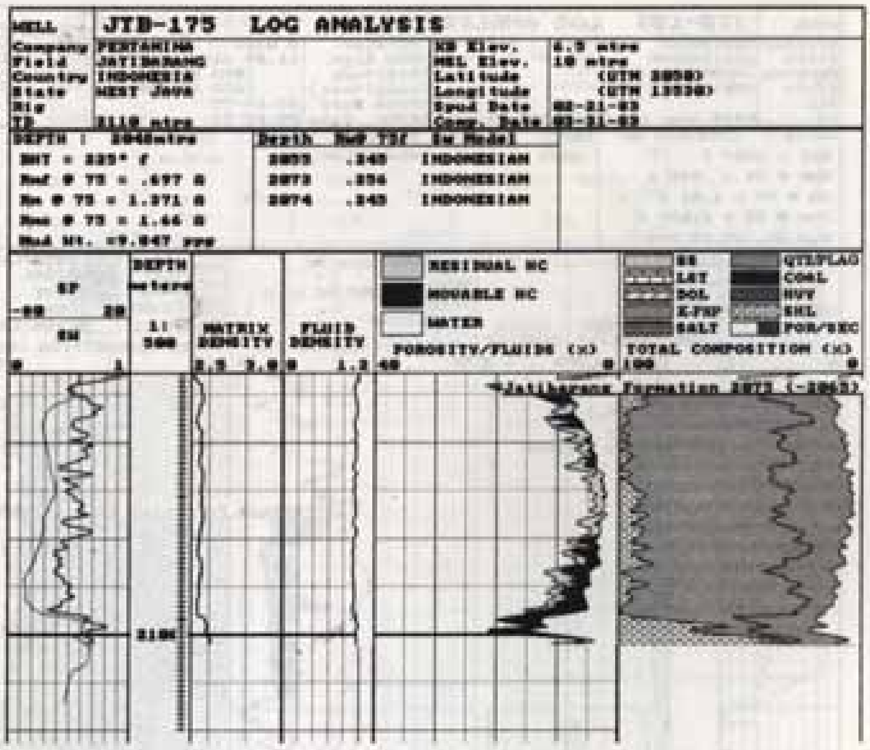

Figure 11. JTB – 175 log analysis results. The top of the shale break within the volcanics is 2098 m. The depth scale is measured depth.

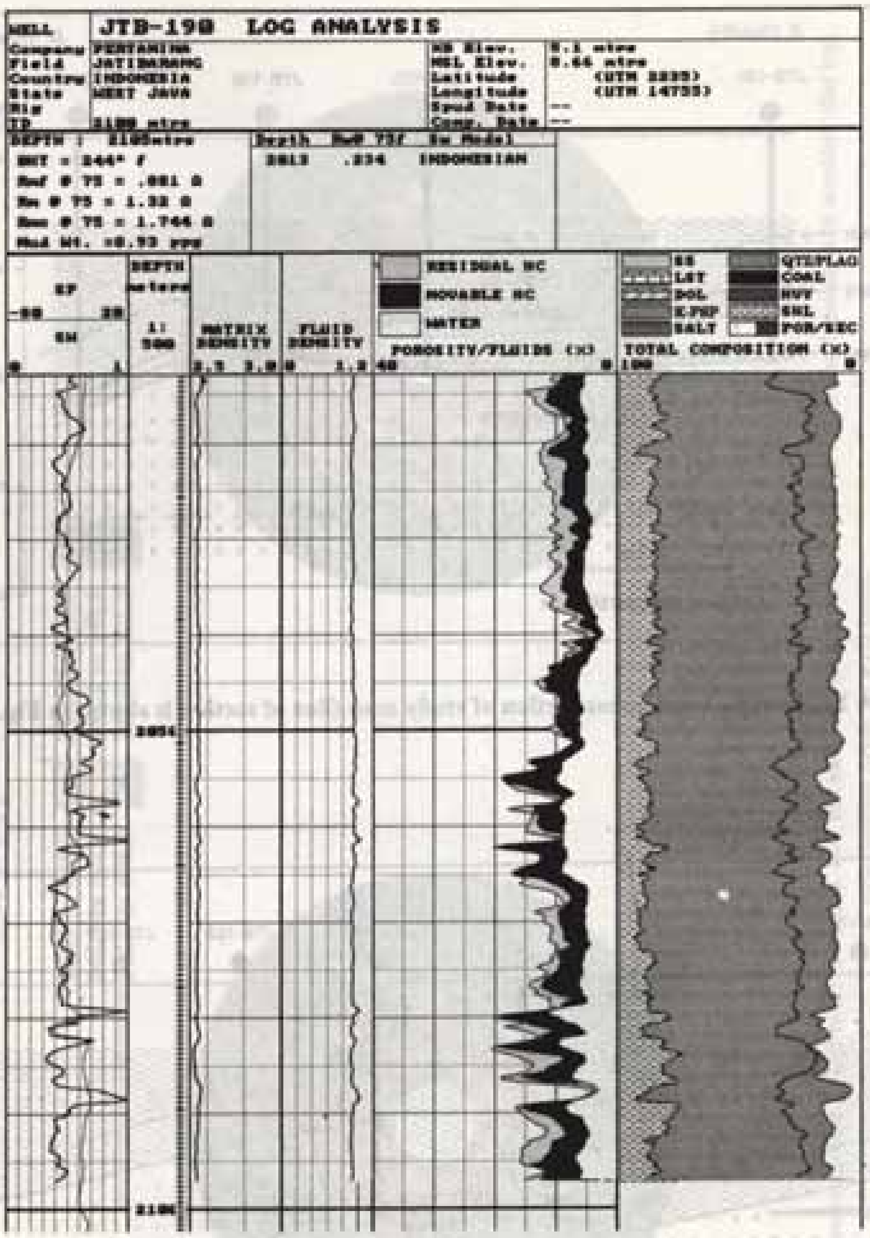

Figure 12. JTB – 190 log analysis results. The depth scale is measured depth.

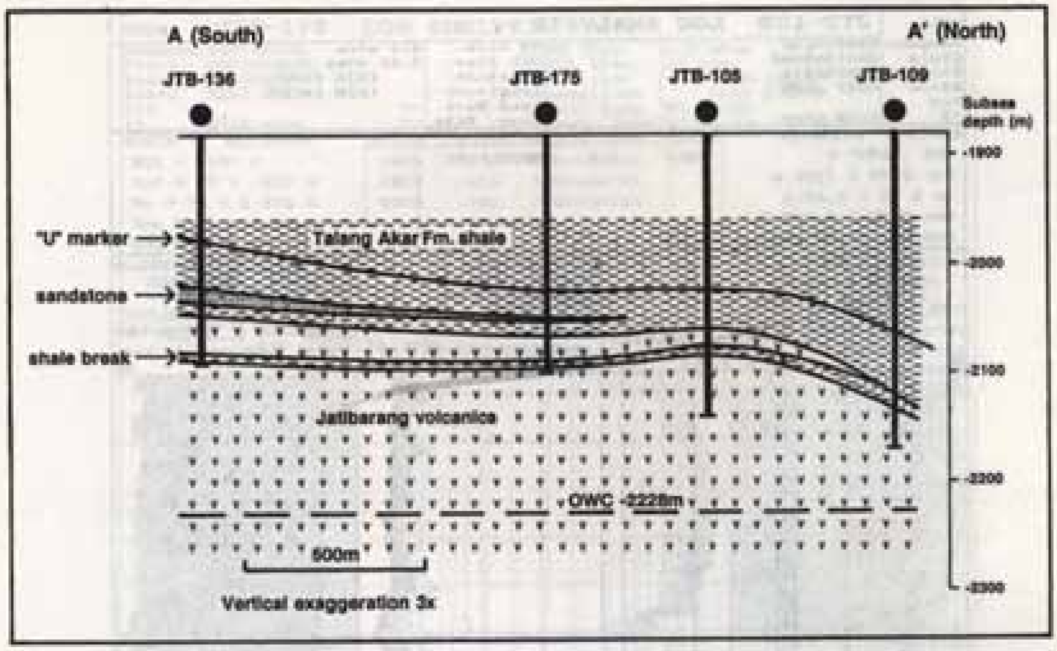

Figure 13. North – south cross section of study area (line of section is shown in Fig. 3)

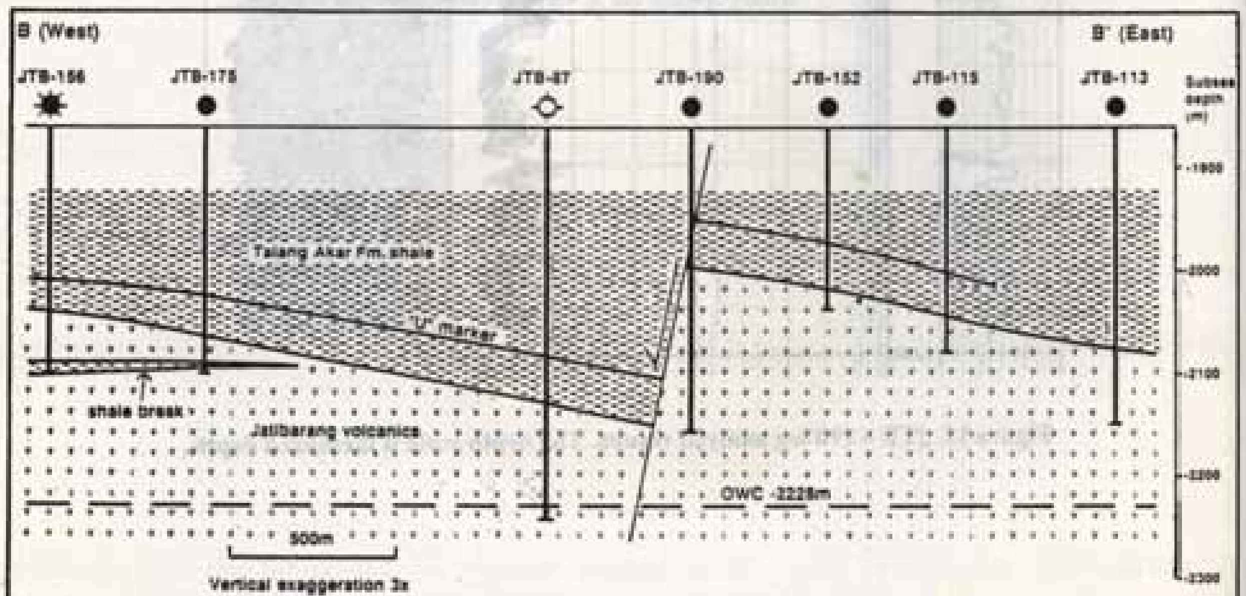

Figure 14. East – west cross section of study area (line of section is shown in Fig. 3)

Figure 15. Pressure response in the matrix blocks and the surrounding fracture system from one time step to another during production prior to well tests.

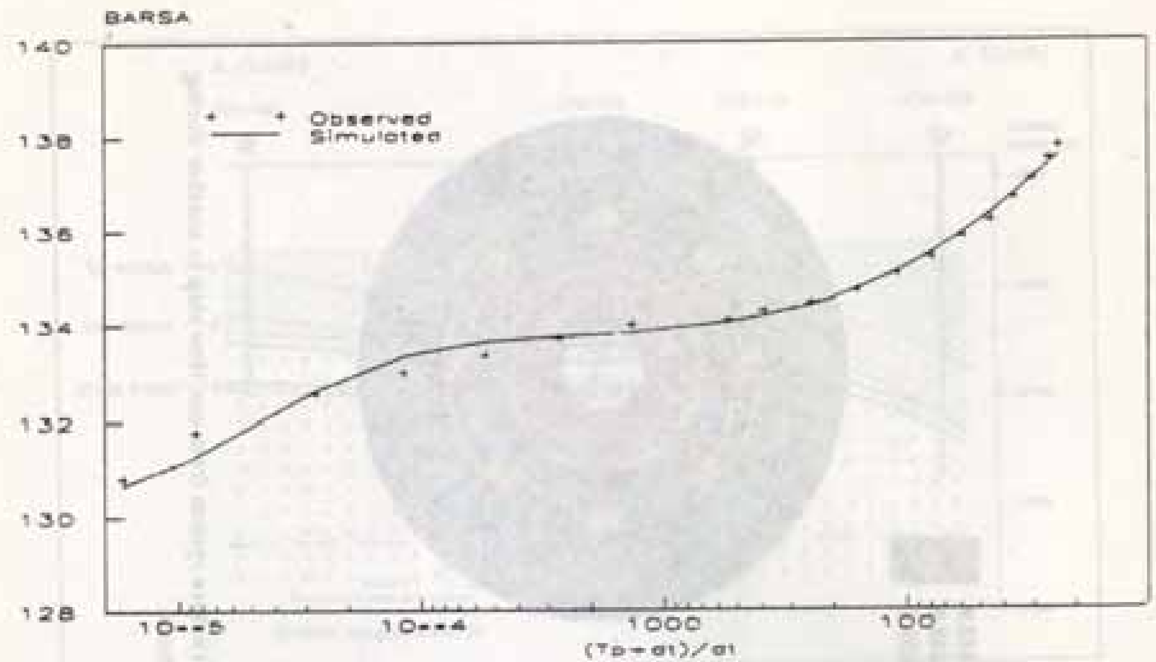

Figure 16. A simulation history match of the build-up pressure data versus dimensionless Horner time in JTB -

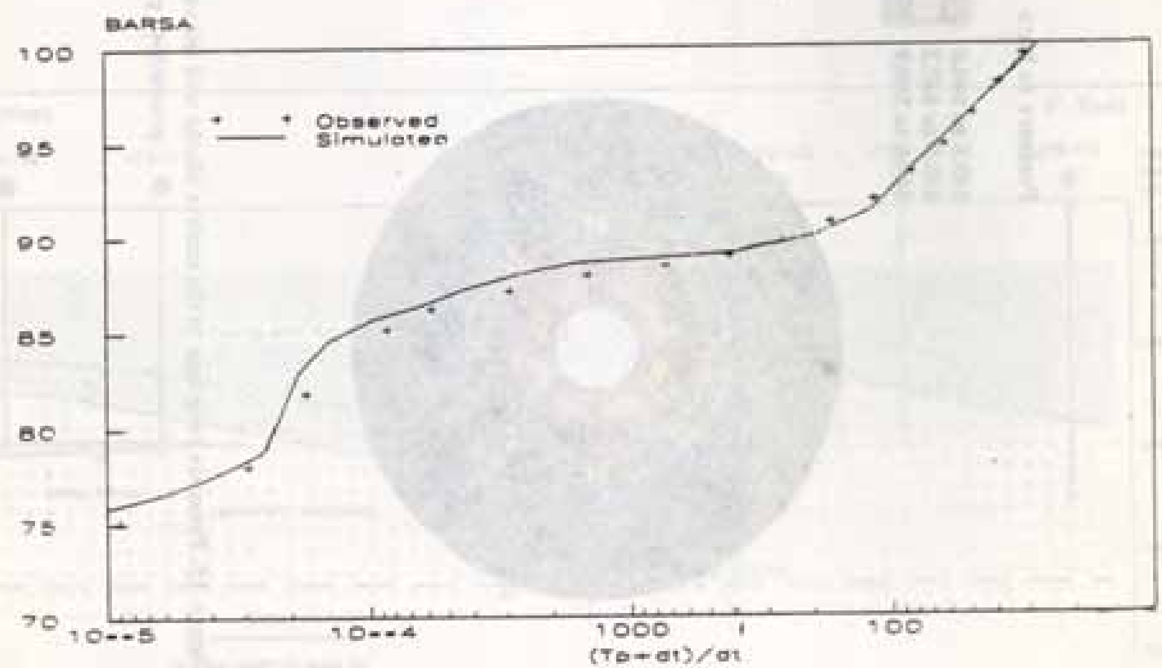

Figure 17. A simulation history match of the build-up pressure data versus dimensionless Horner time in JTB - 17

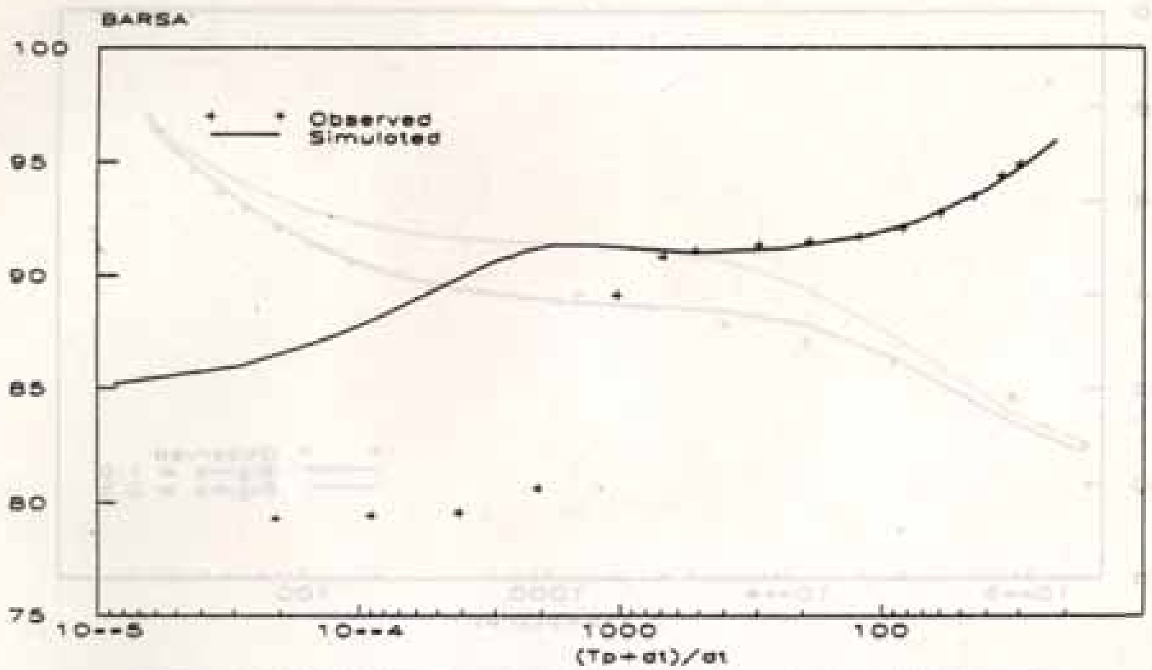

Figure 18. A simulation history match of the build-up pressure data versus dimensionless Horner time in JTB - 190

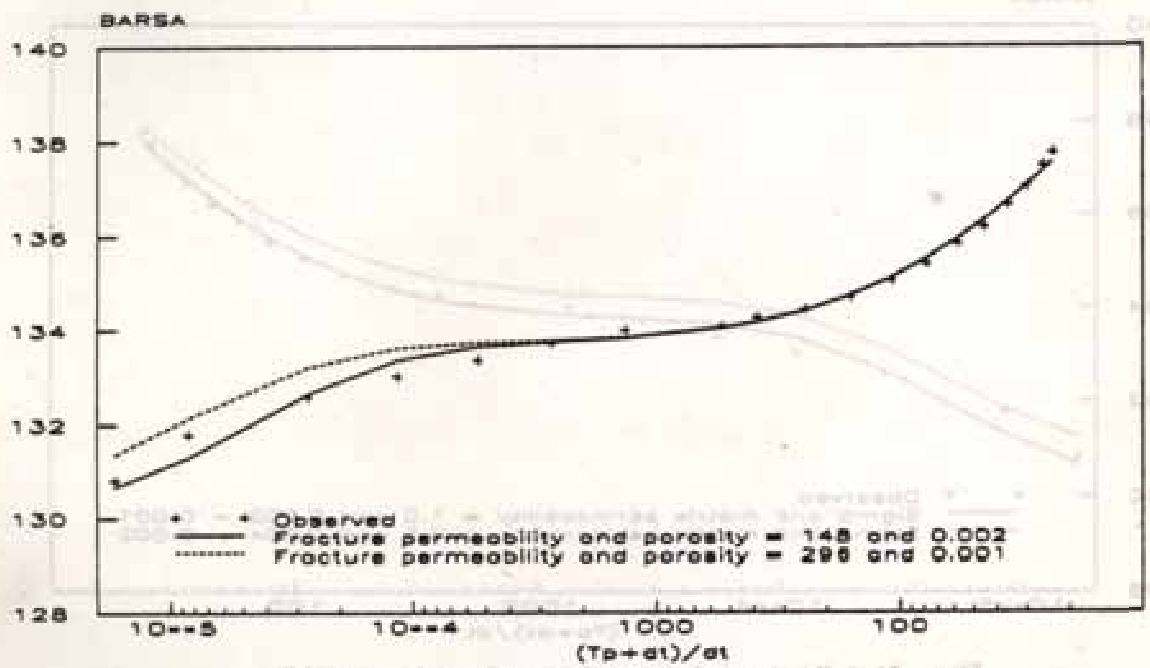

Figure 19. A direct swap between fracture permeability and fracture porosity

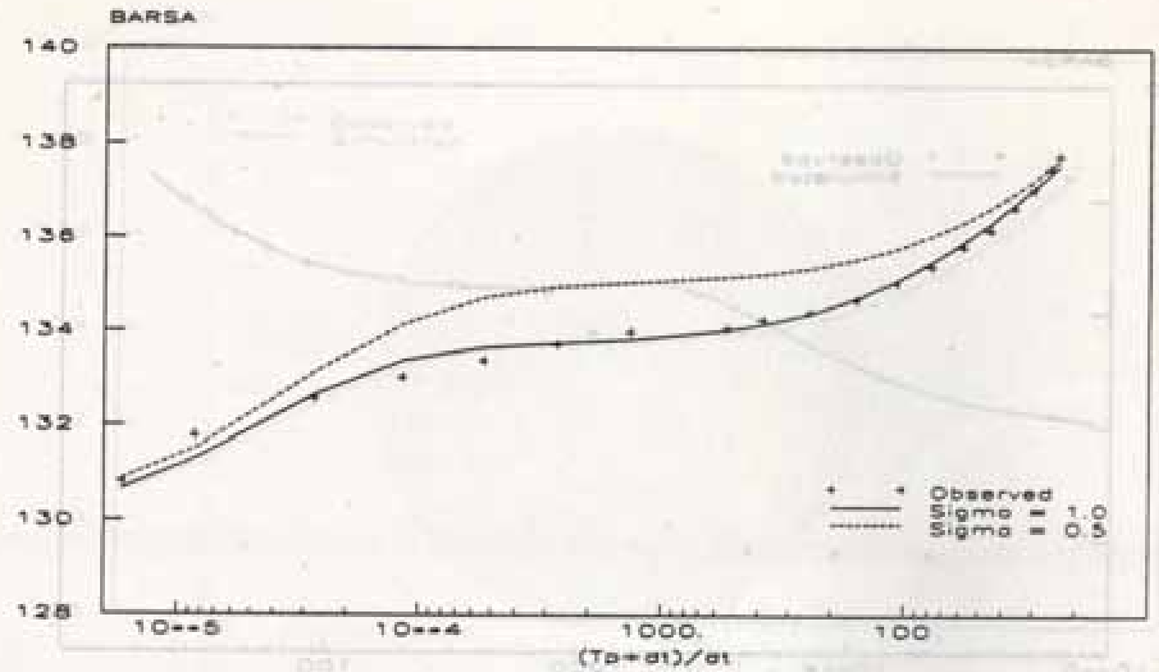

Figure 20. Simulated response to a decrease in sigma compared with the base case

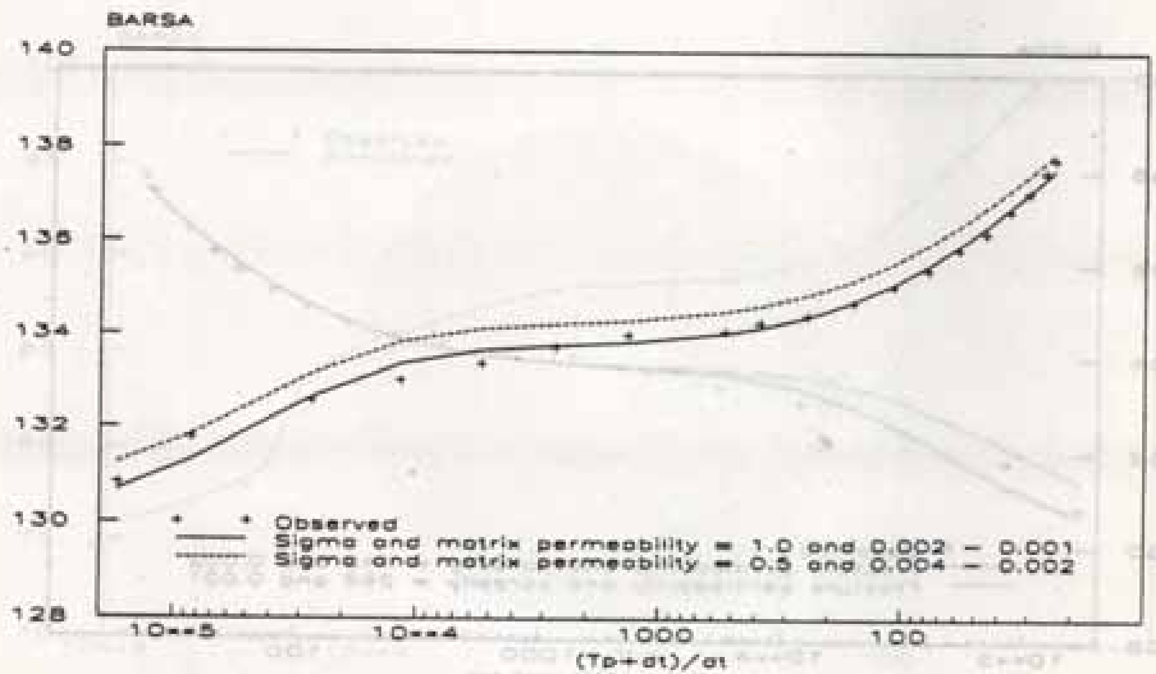

Figure 21. A direct swap between sigma and matrix permeability